Mesoporous Silica Nanoparticles

Generalized Fluorocarbon-Surfactant-Mediated Synthesis of Nanoparticles with Various Mesoporous Structures**

*Yu Han and Jackie Y. Ying**

Research on the synthesis of mesoporous materials has mainly focused on mesostructural diversity,[1–4] compositional flexibility,[5–8] and morphological control.[9–12] The ability to obtain mesoporous particles with a controlled particle size would be important for many practical applications. For example, ultrafine mesoporous particles would be very useful in catalysis and gas adsorption, since they would provide greater pore accessibility and facilitate molecular diffusion. They could also act as the host matrix for the synthesis of quantum dots and magnetic nanoparticles in functional materials and bio-imaging applications.[13] Ultrafine mesoporous particles could also act as carriers for drugs, genes, and proteins for novel biomedical applications.[14,15] Some examples of ultrafine mesoporous particles have been sporadically reported,[16–23] but the type of mesostructure, the degree of structural ordering, and the range of pore sizes are limited. Herein we describe a simple wet-chemical method that enables the synthesis of nanometer-sized particles (50–300 nm) with tunable pore sizes in the range 5–30 nm. This fluorocarbon-surfactant-mediated synthesis can be generalized to achieve various pore structures, including 3D cubic $Im\bar{3}m$, 3D cubic $Fm\bar{3}m$, 2D hexagonal $p6m$, foamlike, and disordered pores, as well as different material compositions.

Our syntheses were carried out in a weakly acidic medium (pH 1.6–1.8), in which a homogeneous solution was formed by mixing a soluble silica precursor, a nonionic triblock copolymer surfactant $EO_xPO_yEO_x$ (EO = ethylene oxide, PO = propylene oxide), and the cationic fluorocarbon surfactant FC-4 ($C_3F_7O(CFCF_3CF_2O)_2CFCF_3CONH(CH_2)_3N^+(C_2H_5)_2-CH_3I^-$). In some cases, the organic swelling agent 1,3,5-trimethylbenzene (TMB) was also added to adjust the pore size or vary the mesostructure. Fluorocarbon surfactants have much higher surface activity than common surfactants. Moreover, unlike the hydrocarbon chains of common surfactants, which are hydrophobic but lipophilic, fluorocarbon chains are hydrophobic and lipophobic. Therefore, hydrocarbon and fluorocarbon surfactants are either immiscible or only partially miscible under most conditions.[24]

In our synthetic strategy, the triblock copolymer surfactant would act as the supramolecular template for the periodic mesostructure, whereas the fluorocarbon surfactant would be used to control the growth of mesoporous particles. The process could be described as follows: The weakly acidic conditions would promote a slow hydrolysis of silica precursors, and the hydrolyzed silica species would co-assemble with triblock copolymer surfactants to form well-defined mesophases, whose structures and pore sizes would depend on the type of copolymer and the amount of organic additives. Simultaneously, fluorocarbon surfactants would surround the silica particles through $S^+X^-I^+$ interactions, thereby limiting the growth of silica particles. By this approach, five different mesoporous structures were successfully obtained with nanometer particle sizes (denoted IBN-1 to IBN-5 in Table 1).

Table 1: Mesoporous nanoparticles obtained with the fluorocarbon-surfactant-mediated synthesis.[a]

Sample	Mesostructure	Template	BET surface area [$m^2 g^{-1}$]	Pore volume [$cm^3 g^{-1}$]	Pore size [nm][b]
IBN-1	3D cubic ($Im\bar{3}m$)	F127	779	0.73	5.8
IBN-2	3D cubic ($Fm\bar{3}m$)	F127 + TMB	804	0.65	9.5
IBN-3	mesocellular foam	P65 + TMB	821	0.72	19.5
IBN-4	2D hexagonal ($p6m$)	P123	709	0.88	6.4
IBN-5	disordered	F108	575	0.54	5.2

[a] Fluorocarbon surfactant FC-4 was used in all syntheses to limit the particle size. [b] Calculated from the adsorption branch of the N_2 sorption isotherm by using the BJH method.

Figure 1a shows an SEM image of calcined IBN-1 that was prepared with Pluronic F127 triblock copolymer ($EO_{106}PO_{70}EO_{106}$) and fluorocarbon surfactant FC-4 by using the synthetic approach described above (see Experimental Section for details). IBN-1 was composed of relatively uniform particles of 100–300 nm. A TEM image (Figure 1a, inset) revealed that these particles are well dispersed with little aggregation. The XRD pattern of calcined IBN-1 (Figure 1e) showed two well-resolved peaks with d spacings of 116 and 82 Å, which could respectively be indexed as the 110 and 200 diffractions of cubic symmetry with a lattice constant of $a = 164$ Å. The high-resolution TEM (HRTEM) images of this material taken at [100], [110], and [111] incidences and the corresponding Fourier transforms (FT) are shown in Figure 1b–d, respectively. IBN-1 particles displayed morphologies that were in good accordance with their cubic symmetry (for example, square and hexagonal particle morphologies were observed in [100] and [111] directions, respectively). The highly ordered arrangement of mesopores that could be observed over the entire particle in all cases indicated the high quality of the sample. The reflections in the FT patterns could be indexed as 110, 200,

[*] Dr. Y. Han, Prof. J. Y. Ying
Institute of Bioengineering and Nanotechnology
31 Biopolis Way, The Nanos, #04-01
Singapore 138669 (Singapore)
Fax: (+65) 6478-9020
E-mail: jyying@ibn.a-star.edu.sg

[**] This work was supported by the Institute of Bioengineering and Nanotechnology (Agency for Science, Technology and Research, Singapore). The authors would like thank Dr. Su Seong Lee and Dr. Yiyan Yang for helpful discussions. They are grateful to BASF Corporation and BASF Singapore for providing the Pluronic triblock copolymer surfactants.

Supporting information for this article is available on the WWW under http://www.angewandte.org or from the author.

  DOI: 10.1002/ange.200460892

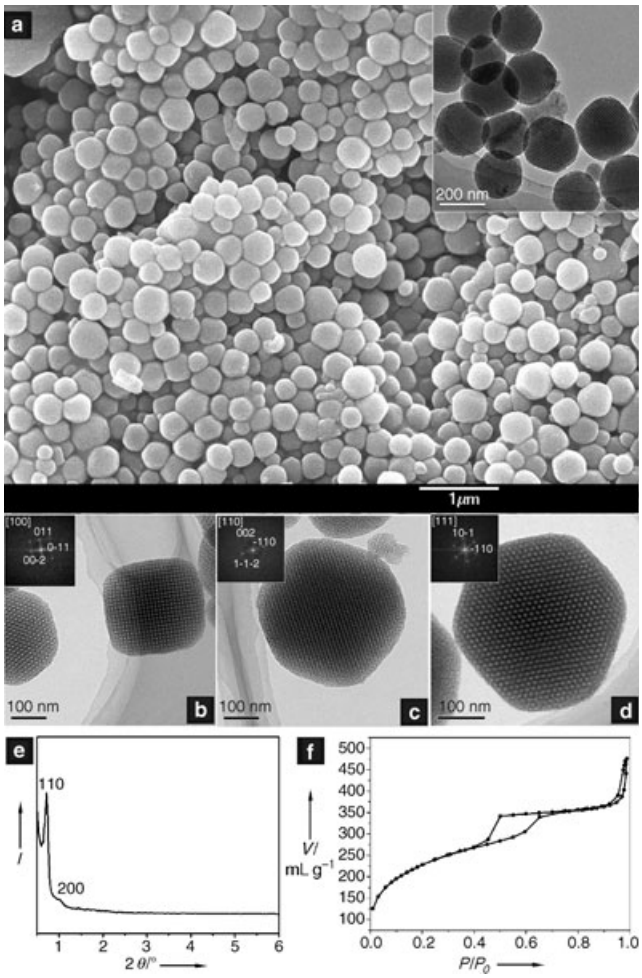

Figure 1. Calcined IBN-1. a) SEM image (inset: TEM image). b)–d) HRTEM images taken at [100], [110], and [111] incidences (insets: the corresponding FT patterns). e) XRD pattern. f) N_2 adsorption/desorption isotherm.

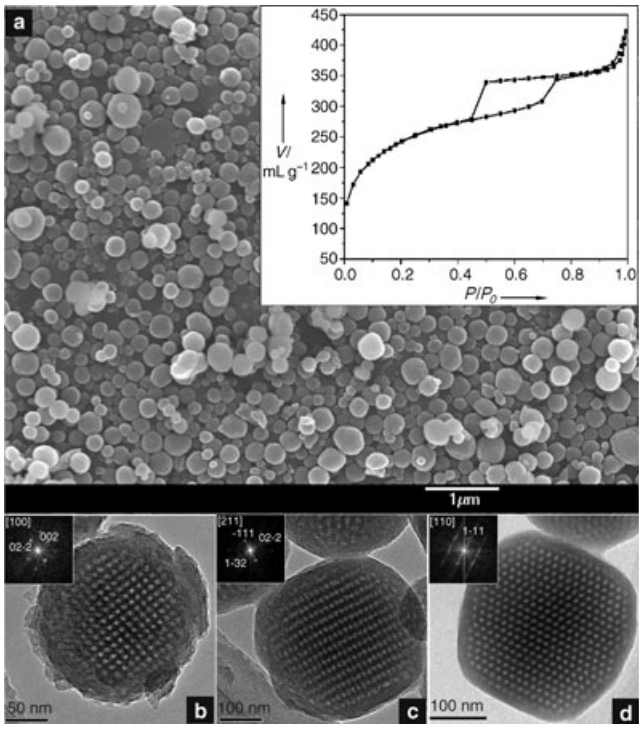

Figure 2. Calcined IBN-2. a) SEM image (inset: N_2 adsorption/desorption isotherm). b)–d) HRTEM images taken at [100], [211], and [110] incidences (inset: corresponding FT patterns).

211, and 220 of a cubic phase ($Im\bar{3}m$ space group) with a large lattice constant of $a = 165$ Å, consistent with the XRD findings. IBN-1 has a type IV N_2 adsorption/desorption isotherm with a type-H_2 hysteresis loop (Figure 1 f), which suggests that the mesopores are cagelike. The average pore diameter was calculated to be 5.8 nm from the adsorption branch of the isotherm by using the Barrett–Joyner–Halenda (BJH) method. Besides the well-defined mesopores, this material showed interparticle (textural) porosity (as evidenced by the adsorption step at high relative pressures of > 0.9), which constituted a quarter of the total pore volume of 0.73 $cm^3 g^{-1}$. IBN-1 has a high BET surface area of 779 $m^2 g^{-1}$.

IBN-2 was synthesized under conditions similar to those for IBN-1, except that a large amount of TMB was added (see Table 1). It is composed of well-dispersed particles of 50–300 nm (Figure 2 a). The N_2 sorption isotherm (Figure 2 a, inset) showed that IBN-2 has cage-type pores averaging 9.5 nm in size, which are much larger than those of IBN-1 due to the addition of TMB as swelling agent. High-resolution TEM images taken at various incidences (Figure 2 b–d) showed well-ordered large pores in IBN-2. The spots in the FT patterns (Figure 2 b–d, insets) were indexed as 111, 200, 220, 311, and 222 reflections of a cubic system with a large lattice constant of $a = 220$ Å. According to extinction rules and previous studies,[25,26] IBN-2 could be assigned to a face-centered cubic structure ($Fm\bar{3}m$). Notably, the FT pattern for [110] incidence showed strong diffuse streaks along the $[1\bar{1}1]$ direction, which suggest the presence of mixed phases. This was confirmed by the corresponding TEM image (Figure 2 d), which illustrated narrow cubic close-packed (ccp, ABCABC…) bands with periodicity in twin relation. In addition, some 3D hexagonal domains with the cages arranged in hexagonal close-packed (hcp, ABAB…) mode were also observed between the cubic twins as a transitional phase (see Supporting Information). This is the first report of an intergrowth of cubic and 3D hexagonal phases in such a small particle; similar intergrowth has been observed in bulk mesoporous silicas such as FDU-1[25] and SBA-12.[26]

Mesocellular foam (MCF) is a novel mesostructured silica material templated by oil-in-water microemulsions.[27,28] The ultralarge mesopores (25–40 nm) have made MCF particularly useful as catalyst support and separation medium for processes involving large substrates. Conventional MCF has a cauliflower-type morphology with a particle size of tens of micrometers.[27] Using our fluorocarbon-surfactant-mediated synthesis, we obtained spherical MCF nanoparticles (50–300 nm), denoted IBN-3 (Figure 3 a). In this synthesis, Pluronic P65 ($EO_{20}PO_{30}EO_{20}$) and TMB were used as the surfactant and oil, respectively, for the formation of a microemulsion template. The ultralarge foamlike pores in the particles obtained could be easily seen by TEM, even at

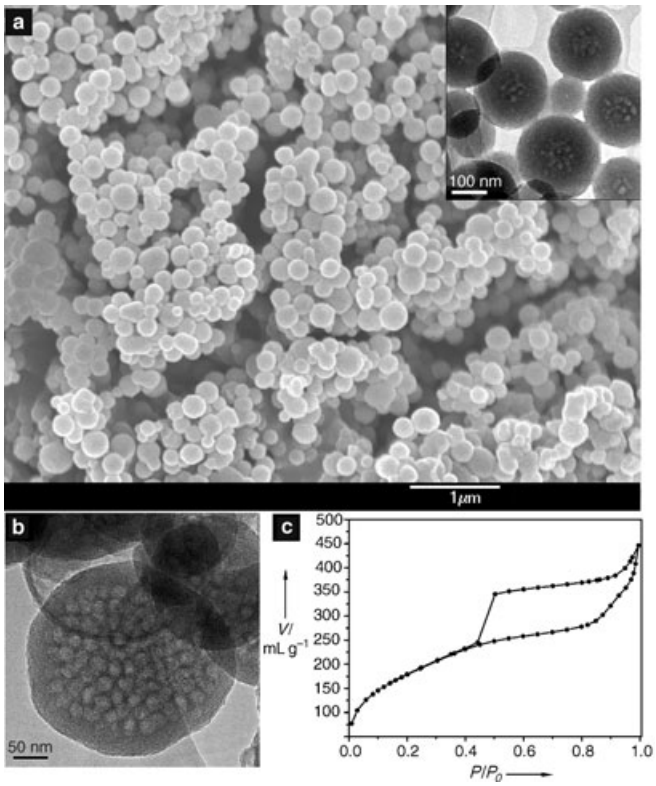

Figure 3. Calcined IBN-3. a) SEM image (inset: TEM image). b) HRTEM image. c) N_2 adsorption/desorption isotherm.

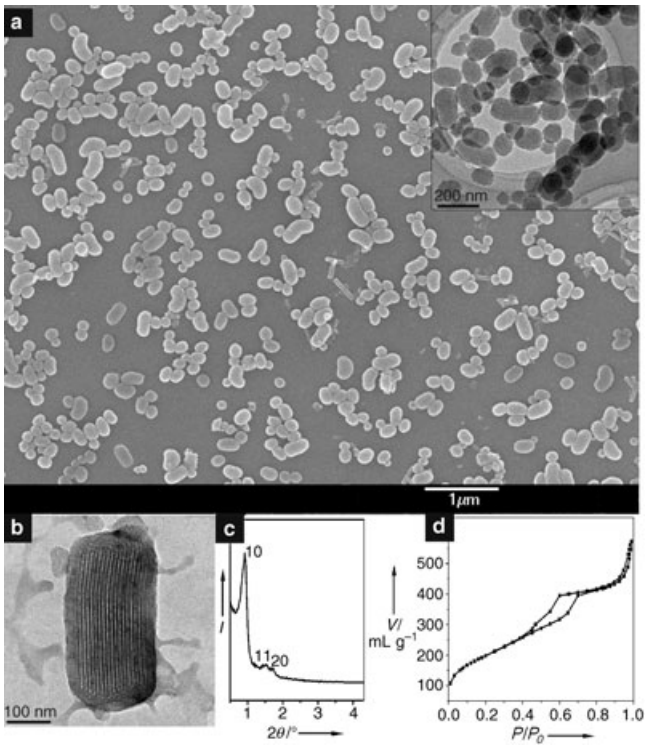

Figure 4. Calcined IBN-4. a) SEM image (inset: TEM image). b) HRTEM image. c) XRD pattern. d) N_2 adsorption/desorption isotherm.

relatively low magnification (Figure 3a, inset). The HRTEM image showed that the pores are about 20 nm in diameter (Figure 3b), consistent with the average adsorption BJH pore size (19.5 nm; Table 1). The pore diameter of IBN-3 could be tailored in the range 15–30 nm, without changing the particle size and morphology, by varying the amount of TMB added in the synthesis.

IBN-1, IBN-2, and IBN-3 all have cage-type mesopores, as evidenced by the type-H_2 hysteresis loops in their sorption isotherms. The fluorocarbon-surfactant-mediated synthesis could also be used to obtain nanoparticles with channel-like mesopores. For example, IBN-4, which was templated by Pluronic P123 ($EO_{20}PO_{70}EO_{20}$), exhibited a mesostructure typical of a 2D hexagonal phase (*p6m*) with a lattice constant of $a = 105$ Å (Figure 4b and c). IBN-4 showed channel-type mesopores with a uniform diameter of 6.4 nm, as calculated from the N_2 sorption isotherm, which has a type-H_1 hysteresis loop (Figure 4d). Most of the IBN-4 particles have a rodlike morphology (200–400 nm long and 50–150 nm wide; Figure 4a), in good accordance with their 2D hexagonal mesostructure.

Periodic mesoporous organosilicas (PMOs) were reported independently in 1999 by three groups.[29–31] We employed 1,2-bis(trimethoxysilyl)ethane and F108 ($EO_{132}PO_{50}EO_{132}$) as precursor and surfactant template, respectively, in our fluorocarbon-surfactant-mediated synthesis to prepare nanoparticles of PMO (IBN-5). The ^{29}Si MAS and ^{13}C CP/MAS NMR spectra (Figure 5d and e) showed that all of the Si atoms in the material are bonded covalently to C atoms and the framework consists of $SiO_{1.5}CH_2CH_2SiO_{1.5}$ structural units. Both SEM and TEM images (Figure 5a and inset) showed that IBN-5 consisted of fairly uniform particles of about 100 nm in size. However, unlike the pure silica materials discussed above, IBN-5 nanoparticles are not well-dispersed. The mesopores in IBN-5 could be observed by TEM, but the contrast was relatively weak (Figure 5a, inset) due to the disordered pore arrangement. Only one peak appeared in the XRD pattern (Figure 5b), a further indication of the lack of long-range order in IBN-5. Nevertheless, the pore size distribution in IBN-5 (centered at ca. 5.2 nm) was still narrow, as illustrated by the sharp step (at $P/P_0 \sim 0.6$) in the adsorption isotherm (Figure 5c). The presence of substantial textural porosity, as judged from the isotherm, revealed that the interparticle voids were still accessible despite the particle agglomeration.

Fluorocarbon surfactant FC-4 was used in all syntheses described above, without which large, irregular mesoporous particles were obtained instead of well-defined nanoparticles. On the other hand, no precipitates were formed if only FC-4 was used without copolymer surfactant. These results illustrate that the use of fluorocarbon surfactant is essential for forming ultrafine particles, while the mesostructures are templated by copolymer surfactant. The function of fluorocarbon surfactant in controlling the particle size is believed to be associated with its special surface activity and immiscibility with copolymer surfactant, which allows them to be enriched at the particle periphery during the particle formation which consequently limits the particle growth. This mechanism is supported by a recent publication which reported the use of a

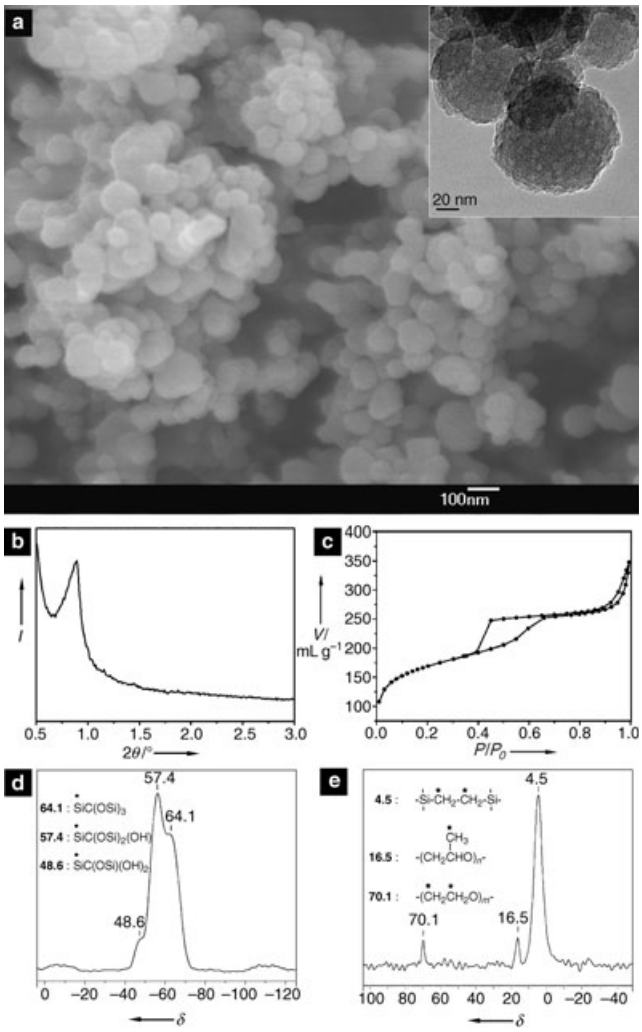

Figure 5. Surfactant-extracted IBN-5. a) SEM image (inset: HRTEM image). b) XRD pattern. c) N_2 adsorption/desorption isotherm. d) ^{29}Si MAS NMR spectrum. e) ^{13}C CP/MAS NMR spectrum (note: the two small peaks at $\delta = 16.5$ ppm and 70.1 ppm were due to C species from residual triblock copolymer surfactant).

mixture of copolymer F127 and cationic fluorocarbon surfactant IC-11 to obtain a new core–shell structure in silica particles.[22] In that study, IC-11 and F127 gave rise to the mesoporosity in the shell and the mesoporosity in the core, respectively, due to the phase separation of fluorocarbon surfactant from copolymer surfactant, with ordered packing of fluorocarbon surfactant around the silica particles. In our case, however, the FC-4 micelles were most likely packed around the silica particles in a disordered manner, since no ordered pattern was observed at the edge of the particles.

The optimal ratio of FC-4 to copolymer surfactant for nanoparticle synthesis depends on the nature of the copolymer. For example, when the concentration of FC-4 was kept within 2.0–2.5 wt%, as used in our syntheses, the triblock copolymers with relatively long hydrophilic EO segments [for example, F127 ($EO_{106}PO_{70}EO_{106}$) and F108 ($EO_{132}PO_{50}EO_{132}$)] could be used over a wide range of concentrations (0.5–3 wt%) to produce IBN-1 and IBN-5, respectively. In contrast, the triblock copolymer with low EO/PO ratio [for example, Pluronic P123 ($EO_{20}PO_{70}EO_{20}$)] had to be used at low concentrations (0.5–1 wt%) in the synthesis of IBN-4, or large particles with an irregular morphology were obtained. This was possibly because different copolymers have different miscibilities with FC-4.[32–34] In general, the longer its hydrophobic PO segment, the more solubilizing power the triblock copolymer has, and therefore the more likely it would form mixed micelles with fluorocarbon surfactant.[32] Thus, a copolymer surfactant with a large hydrophobic volume (for example, P123), would involve most of the FC-4 molecules in forming mixed micelles at relatively high concentrations, but when its concentration was kept low, excess FC-4 molecules would still contribute to controlling particle growth.[34] For cases that involve TMB addition (for example, IBN-2 and IBN-3), low concentrations of copolymer should be used, since TMB will increase the hydrophobic volume of the copolymer micelles, and consequently increase the tendency to form mixed micelles with FC-4.

Moreover, mildly acidic conditions (pH 1.6–1.8) and a moderate reaction temperature (25–30 °C) were necessary for the syntheses. Stronger acidity or higher temperature would promote a rapid, uncontrolled hydrolysis/condensation of silica species which would not lead to the formation of ultrafine particles with a regular morphology. Weaker acidity with a pH value above 2.0 would not promote the co-assembly of surfactant and silica species, and lower reaction temperature would result in materials with poorly ordered mesostructures.

Experimental Section

IBN-1: 0.65 g of Pluronic F127 and 0.8 g of FC-4 were dissolved in 40 mL of aqueous HCl solution (0.02 M), and 2.2 g of tetraethyl orthosilicate (TEOS) was added. The solution was stirred at 30 °C for 20 h, and then transferred to an autoclave for further condensation at 100 °C for 1 d. The product was collected by centrifugation, dried in air, and calcined at 550 °C for 5 h for surfactant removal. Details on the syntheses of other mesoporous nanoparticles are described in the Supporting Information.

XRD patterns were obtained with a Siemens D5005 diffractometer by using $Cu_{K\alpha}$ radiation. SEM images were obtained on a JEOL JSM-6700F electron microscope. TEM experiments were performed on a JEOL JEM-3010 electron microscope with an acceleration voltage of 300 kV. The nitrogen sorption isotherms were obtained with a Micromeritics ASAP 2020M system; the samples were degassed for 10 h at 150 °C before the measurements. ^{29}Si and ^{13}C CP/MAS NMR spectra were recorded with a Bruker AV500WB system with a 4 mm DVT CP/MAS probe; chemical shifts for both spectra were referenced to tetramethylsilane (TMS) at 0 ppm.

Received: June 7, 2004

Keywords: hydrothermal synthesis · mesoporous materials · nanoparticles · silica

[1] Q. Huo, D. I. Margolese, U. Ciesla, P. Feng, T. E. Gier, P. Sieger, R. Leon, P. M. Petroff, F. Schüth, G. D. Stucky, *Nature* **1994**, *368*, 317.

[2] Y. Sakamoto, M. Kaneda, O. Terasaki, D. Zhao, J.-M. Kim, G. D. Stucky, H. J. Shin, R. Ryoo, *Nature* **2000**, *408*, 449.

[3] D. Zhao, Q. Huo, J. Feng, B. F. Chmelka, G. D. Stucky, *J. Am. Chem. Soc.* **1998**, *120*, 6024.
[4] J. Y. Ying, C. P. Mehnert, M. S. Wong, *Angew. Chem.* **1999**, *111*, 58; *Angew. Chem. Int. Ed.* **1999**, *38*, 56.
[5] B. Tian, X. Liu, B. Tu, C. Yu, J. Fan, L. Wang, S. Xie, G. D. Stucky, D. Zhao, *Nat. Mater.* **2003**, *2*, 159.
[6] D. M. Antonelli, J. Y. Ying, *Angew. Chem.* **1996**, *108*, 461; *Angew. Chem. Int. Ed. Engl.* **1996**, *35*, 426.
[7] F. Schüth, *Chem. Mater.* **2001**, *13*, 3184.
[8] R. Ryoo, S. H. Joo, S. Jun, *J. Phys. Chem. B* **1999**, *103*, 7743.
[9] S. Schacht, Q. Huo, I. G. Voigt-Martin, G. D. Stucky, F. Schüth, *Science* **1996**, *273*, 768.
[10] P. J. Bruinsma, A. Y. Kim, J. Liu, S. Baskaran, *Chem. Mater.* **1997**, *9*, 2507.
[11] H. Yang, N. Coombs, I. Sokolov, G. Ozin, *Nature* **1996**, *381*, 589.
[12] I. A. Aksay, M. Trau, S. Mann, I. Honma, N. Yao, L. Zhou, P. Fenter, P. M. Eisenberger, S. M. Gruner, *Science* **1996**, *273*, 892.
[13] J. Y. Ying, *Sci. Spectra* **1999**, *18*, 56.
[14] C.-Y. Lai, B. G. Trewyn, D. M. Jeftinija, K. Jeftinija, S. Xu, S. Jeftinija, V. S.-Y. Lin, *J. Am. Chem. Soc.* **2003**, *125*, 4451.
[15] Y.-J. Han, G. D. Stucky, A. Butler, *J. Am. Chem. Soc.* **1999**, *121*, 9897.
[16] K. Suzuki, K. Ikari, H. Imai, *J. Am. Chem. Soc.* **2004**, *126*, 462.
[17] S. Sadasivan, F. E. Fowler, D. Khushalani, S. Mann, *Angew. Chem.* **2002**, *114*, 2255; *Angew. Chem. Int. Ed.* **2002**, *41*, 2151.
[18] Q. Cai, Z.-S. Luo, W.-Q. Pang, Y.-W. Fan, X.-H. Chen, F.-Z. Cui, *Chem. Mater.* **2001**, *13*, 258.
[19] R. I. Nooney, D. Thirunavukkarasu, Y. Chen, R. Josephs, A. E. Ostafin, *Chem. Mater.* **2002**, *14*, 4721.
[20] W. Zhao, Q. Li, *Chem. Mater.* **2003**, *15*, 4160.
[21] Y. Lu, H. Fan, A. Stump, T. L. Ward, T. Rieker, C. J. Brinker, *Nature* **1999**, *398*, 223.
[22] S. Areva, C. Boissière, D. Grosso, T. Asakawa, C. Sanchez, M. Lindén, *Chem. Commun.* **2004**, 1630.
[23] D. Grosso, E. L. Crepaldi, B. Charleux, C. Sanchez, *Adv. Funct. Mater.* **2003**, *13*, 37.
[24] M. Almgren, K. Wang, *Langmuir*, **1997**, *13*, 4535.
[25] J. R. Matos, M. Kruk, L. P. Mercuri, M. Jaroniec, L. Zhao, T. Kamiyama, O. Terasaki, T. J. Pinnavaia, Y. Liu, *J. Am. Chem. Soc.* **2003**, *125*, 821.
[26] Y. Sakamoto, I. Diaz, O. Terasaki, D. Zhao, J. Perez-Pariente, J. Kim, G. D. Stucky, *J. Phys. Chem. B* **2002**, *106*, 3118.
[27] P. Schmidt-Winkel, P. Yang, D. I. Margolese, J. S. Lettow, J. Y. Ying, G. D. Stucky, *Chem. Mater.* **2000**, *12*, 686.
[28] J. S. Lettow, Y. J. Han, P. Schmidt-Winkel, P. Yang, D. Zhao, G. D. Stucky, J. Y. Ying, *Langmuir* **2000**, *16*, 8291.
[29] T. Asefa, M. J. MacLachlan, N. Coombs, G. A. Ozin, *Nature* **1999**, *402*, 867.
[30] S. Inagaki, S. Guan, Y. Fukushima, T. Ohsuna, O. Terasaki, *J. Am. Chem. Soc.* **1999**, *121*, 9611.
[31] B. J. Melde, B. T. Holland, C. F. Blanford, A. Stein, *Chem. Mater.* **1999**, *11*, 3302.
[32] N. Funasaki, S. Hada, *J. Phys. Chem.* **1983**, *87*, 342.
[33] Y. Muto, K. Esumi, K. Meguro, R. Zana, *J. Colloid Interface Sci.* **1987**, *120*, 162.
[34] Y. Han, D. Li, L. Zhao, F.-S. Xiao, *Angew. Chem.* **2003**, *115*, 3761; *Angew. Chem. Int. Ed.* **2003**, *42*, 3633.

